

High recognition accuracy tactile sensor based on boron nitride nanosheets/epoxy composites for material identification

Shufen Wang^{a*}, Mengyu Li^a, Hailing Xiang^a, Wenlong Chen^a, Ruping Xie^a, Zhixiong Lin^a,

Konghong Hu^a, Ning Zhang^{b*} and Chengmei Gui^{c*}

^a School of Energy Materials and Chemical Engineering, Hefei University, Hefei City, 230601, China

^b School of Mechanical Engineering, Guizhou University of Engineering Science, Bijie City, 551700, China

^c School of Chemistry and Chemical Engineering, Chaohu University, Hefei City, 230009, China

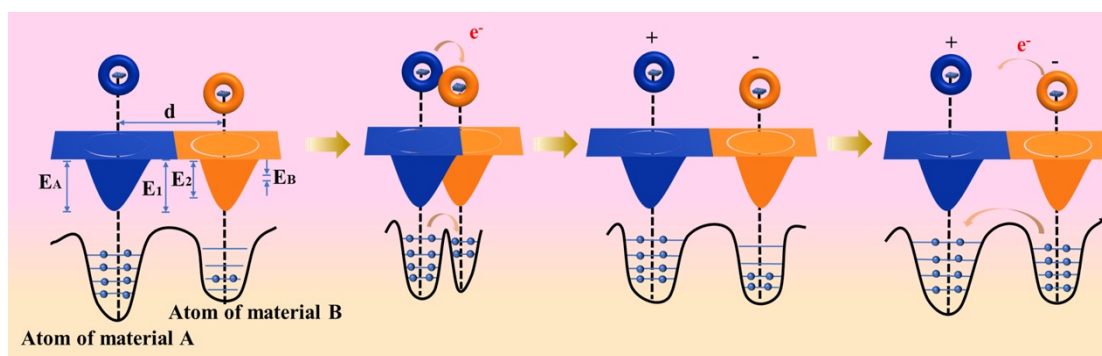


Fig. S1. An overlapping electron cloud model elucidating the fundamental principles of the TENG .

It can be theorized that friction electrical sensing is suitable for the detection of all types of materials. Contact electrification is a fundamental phenomenon that exists at various contact interfaces, and the phenomenon can be explained by the electron cloud overlap model, which depicts two materials in contact at the atomic scale, as shown in Fig. S1. Before this, the respective electron clouds are independent of each other and do not overlap. In the absence of electron transfer, potential wells are capable of binding electrons to specific orbitals with a high degree of stability. When two atoms come into contact, their electron clouds overlap to form a bond. The application of an external force, such as friction or pressure, results in a reduction in bond length, leading to a transition from an initial single-well potential to an asymmetric double-well potential. The strong overlap of electron clouds results in a

weakening of the energy barrier between atoms, thereby facilitating the transfer of electrons from one atom to another. The friction electric signal between two given materials is distinctive due to the variation in electron cloud states across different materials.

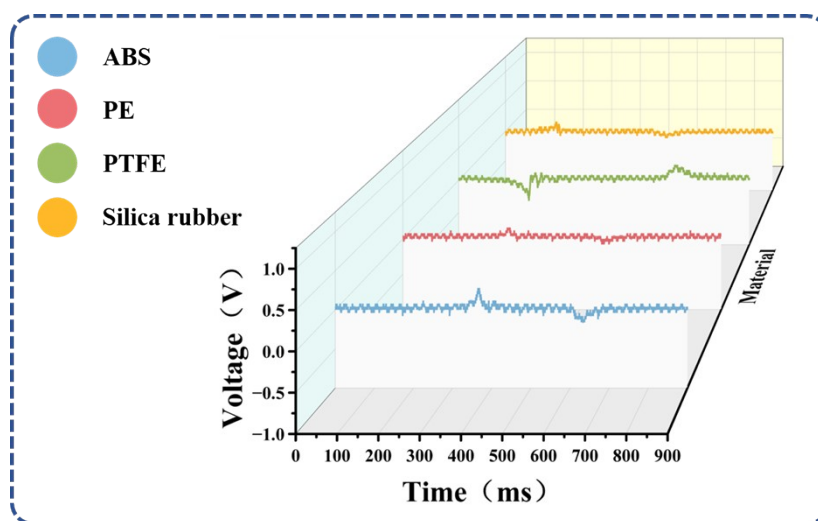


Fig. S2. Analysis of the output waveform signal.

To more clearly illustrate the impact of PDMS on the identification of the materials used, we constructed a straightforward single-electrode TENG device utilizing PDMS as the negative electrode and ABS, PE, PTFE, and Silica rubber as the positive electrode, respectively. The resulting output waveforms were then captured using an oscilloscope (Fig. S2). By comparing with the output waveform in Fig. 5b, it can be seen that the TENG with PDMS as the negative electrode does not perform as well in recognizing the eight materials. This also verifies the superiority of the performance of our materials in the previous section.

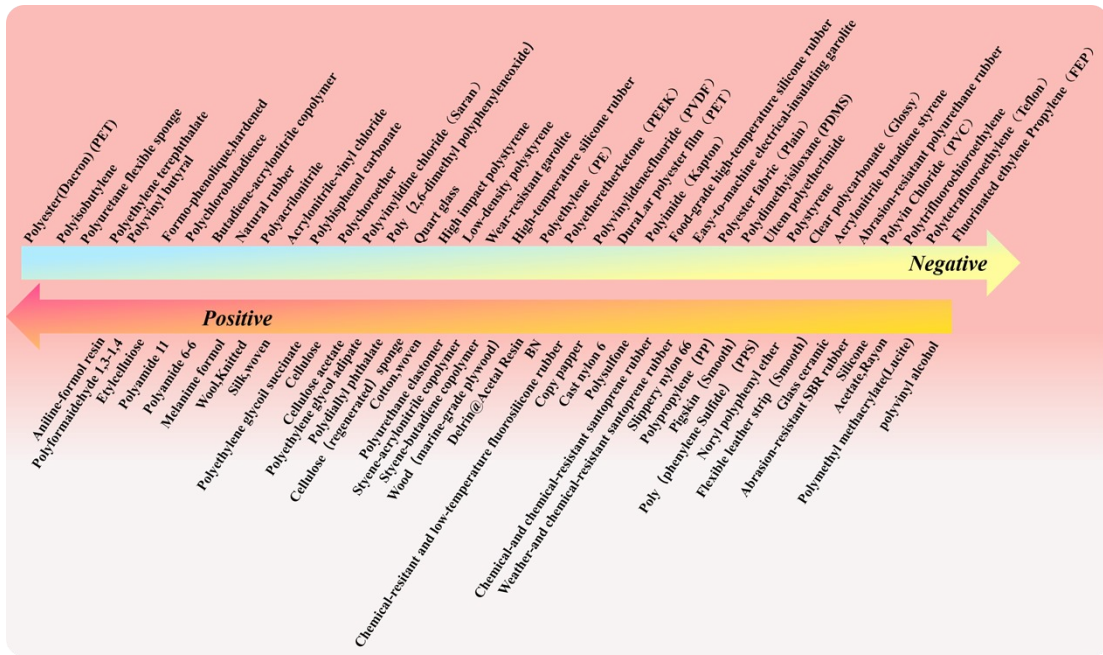


Fig. S3. Friction electric sequence for different materials.

It is well established that the propensity for gaining and losing electrons varies significantly between different materials. The electric sequence table of friction, presented in Fig. S3, was developed based on the observed trends in electron gain and loss across a range of materials. The data presented in this chart illustrates that the material located in the upper right quadrant exhibits a greater electron affinity than the material situated in the lower left quadrant. This implies that the former possesses a superior capacity to gain electrons, rendering it an optimal choice as a negative friction material. Conversely, the material in the lower left quadrant demonstrates a greater ability to lose electrons, making it an ideal candidate for implementation as a positive friction material. From the aforementioned evidence, it can be discerned that when two materials that are situated at considerable distances from one another come into contact, the material located in the lower left quadrant releases electrons, which are then transferred to the material situated in the upper right quadrant. This results in the surfaces of the two materials acquiring an opposite charge. When the two

materials are separated, an electric potential is thereby created.

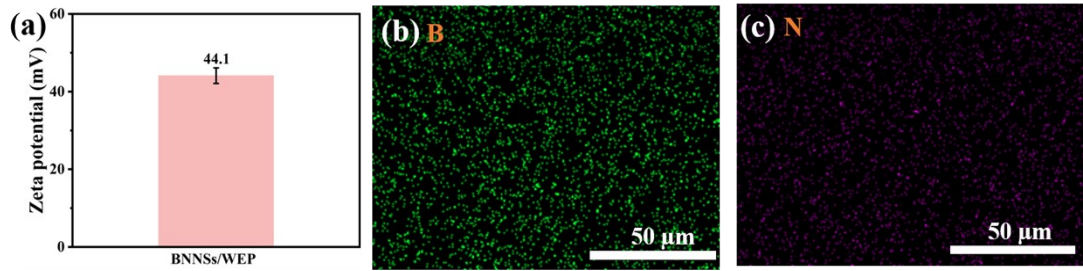


Fig. S4 (a) Zeta potential of BNNs/WEP latex; (b-c) B and N elements mapping of BNNs/WEP composite.

Fig. S4 (a) illustrates the results of the zeta potential test of BNNs/WEP latex, which was used to assess the dispersion stability of the latex. The results showed that the zeta potential of BNNs/WEP latex was 44.1 mV, which was much higher than the stability threshold of 30 mV, confirming the excellent dispersion stability of the latex system. The B and N elemental mappings of BNNs/WEP composites (Fig. S4 b-c), revealed that the distribution of B and N elements on the surface of BNNs/WEP composites are uniform.

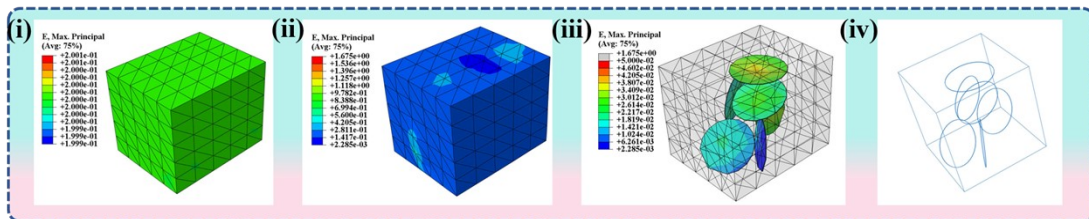
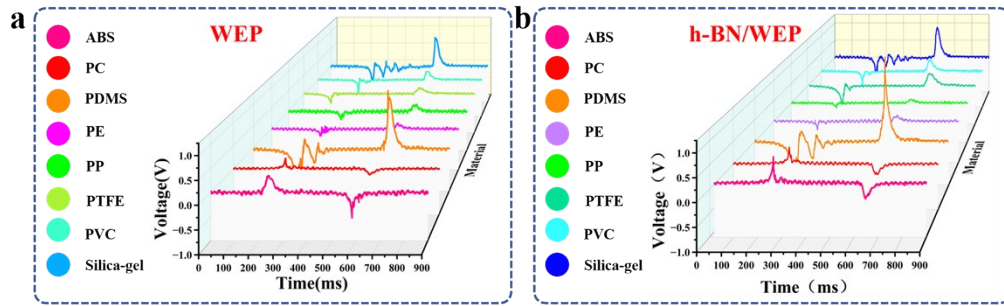


Fig. S5 Strain analysis of friction electric materials during compression

To analyze the stress and strain distribution of friction electric materials in greater detail when subjected to a uniform external load, we employ the finite element periodic boundary load RVE volume element method and simulate it with the assistance of Tor Abaqus software. This enables us to explore the stress and strain of different friction electric materials under identical loading conditions. Fig. S5 illustrates the strain results of the two friction electric materials. It can be observed that the incorporation of BNNs (Fig. S5 i-iv) markedly enhances the strain properties of the materials in comparison to the epoxy resin (Fig. S5 i). Moreover, this outcome

aligns with the observations presented in Fig. 3c. The 1wt% BNNSs/WEP model generated using Abaqus has a length, width and height of 1 μm and comprises 6 rings representing BNNSs(Fig. S5 iv and Fig. 3b i). In this example, the mass fraction of BNNS in the BNNSs/WEP composite is 1%, the density of the epoxy resin (ρ_E) is 1.2 g/cm^3 . According to the previous characterization results, the radius of BNNSs is about 250 nm, the average thickness is 4.5 nm, and the density (ρ_B) is 2.29 g/cm^3 . Therefore, the number of BNNSs was calculated to be 6. By analyzing the stress and strain of the friction electrodes (Fig. 3b, Fig. S5), it can be seen that the stress and strain performance of the friction electrode with BNNSs/WEP composites is much better than that of epoxy resins.



c

Object	WEP		h-BN/WEP		BNNSSs/WEP	
	Peak I	Peak II	Peak I	Peak II	Peak I	Peak II
Silica rubber	0.80	0.84	0.8	0.88	1.42	0.96
PVC	0.38	0.24	0.44	0.32	1.08	0.60
PP	0.24	0.18	0.14	0.10	0.76	0.34
PE	0.20	0.14	0.22	0.16	0.62	0.48
PDMS	1.76	1.32	1.80	1.96	1.54	1.14
PC	0.24	0.14	0.38	0.38	1.36	0.64
ABS	0.36	0.54	0.68	0.22	0.84	0.46
PTFE	0.24	0.20	0.61	0.35	0.5	0.24

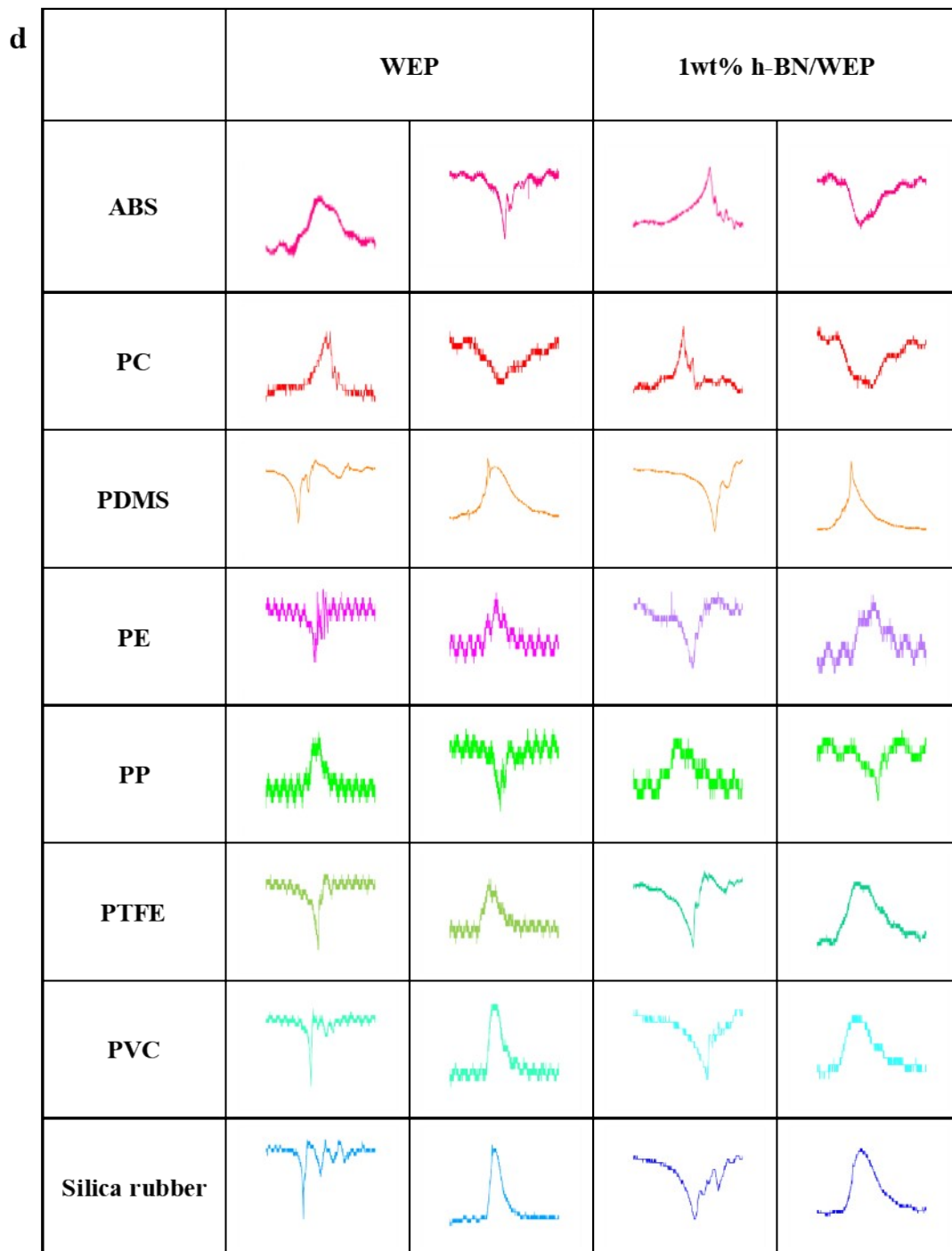


Fig. S6. Analysis and analogy of output waveform of TENG devices fabricated based on different materials. (a) Waveform diagrams of WEP identifying eight different materials. (b) Waveform diagrams of BNNSs/WEP identifying eight different materials. (c) The output voltage of TENG devices with WEP, h-BN/WEP, and BNNSs/WEP for identifying eight different materials. (d) Peak shape diagrams for WEP and h-BN/WEP identifying eight different materials.

As demonstrated in the preceding section, the accuracy of our proposed TENG device recognition is contingent upon the distinctiveness of the extracted features of

the recognized material. Additionally, the peak-to-valley intervals, minimum-to-maximum values, maximum values, and other such metrics also influence the accuracy of the material recognition. It is thus possible to analyze the advantages and disadvantages of the performance of TENG devices from these aspects. In this study, we compare the output waveforms of TENG devices fabricated using three materials (WEP, 1wt% h-BN/BNNSs, and 1wt% BNNSs/WEP) for eight materials, as well as their voltage maxima and minima. This analysis aims to identify the advantages and disadvantages of TENG device performance based on these three materials. By comparing Figs. S6 (a-b) with Fig. 5b we can see that the output signals of 1wt% BNNSs/WEP composite film are more pronounced compared to WEP and 1wt% h-BN/BNNSs composite film, and by specifically analyzing the voltage peaks output from the three materials (Fig. S6 c), it can be seen that the 1wt% BNNSs/WEP composite film has the largest voltage peaks, except when the identified materials are PDMS and PTFE. TENG device based on 1wt% BNNSs/WEP composite film has the largest voltage peak. Furthermore, a comparison of the features of the peaks in Fig. 5d and Fig. S6d reveals that the characteristics from TENG device based on 1wt% BNNSs/WEP are more pronounced and distinct. This facilitates the differentiation of the materials when constructing the machine learning model, thereby indirectly enhancing the accuracy of material recognition.